Electronic Supplementary Information

Measuring metal halide perovskite single cell degradation consistent with module-based conditions.

Robert Tirawat,*[a] Amy E. Louks,[b,d] Mengjin Yang,[b] Severin N. Habisreutinger,[a] Jao van de Lagemaat,[a] Soňa Uličná,[a] Ross A. Kerner,[a] Kai Zhu,[a] Laura T. Schelhas,[a] Axel F. Palmstrom,[b] Joseph J. Berry *[b,c]

[a] *Chemistry and Nanoscience Center, National Renewable Energy Laboratory, Golden, Colorado 80401, USA. E-Mail: Robert.Tirawat@nrel.gov*

[b] *Materials Science Center, National Renewable Energy Laboratory, Golden, Colorado 80401, USA. E-Mail: Joe.Berry@nrel.gov*

[c] *Department of Physics University of Colorado, Boulder Colorado 803009. Renewable and Sustainable Energy Institute, University of Colorado, Boulder, Colorado 80309*

[d] *Department of Chemistry, Colorado School of Mines, Golden, CO, 80401, USA.*

Experimental Procedures

Materials

Substrates are 25 mm × 25 mm patterned indium-doped tin-oxide coated soda lime glass (< 20 Ω/sq) acquired from Colorado Concept Coatings. A Nickle oxide sputtering target (99.9%) and silver pellets (99.99%) were purchased from Kurt J. Lesker. Poly(triaryl amine) (PTAA), cesium iodide (99.999%), N,N-dimethylformamide (anhydrous, 99.8%) (DMF), 1-methyl-2-pyrrolidinone (anhydrous, 99.5%) (NMP), and toluene (anhydrous, 99.8%) were purchased from Sigma-Aldrich. Lead(II) iodide (99.99%), lead(II) bromide (<98.0%), and bathocuproine (purified by sublimation) (BCP) were purchased from TCI Chemicals. Methylammonium bromide (CH_3NH_3Br) and formamidinium iodide (CH_5IN_2) were purchased from Greatcell Solar Materials. C_{60} (>99.5%) was purchased from Luminescence Technology Corp.

Device fabrication

Devices were prepared on indium-doped tin oxide (ITO)-coated glass substrates. The substrates were mechanically cleaned with a sonic toothbrush with Liquinox detergent before sequential ultrasonic baths in detergent, deionized water, acetone, and isopropanol. The cleaned substrates were UV-ozone treated in dry air for 15 minutes immediately before deposition of the nickel oxide layer. A 5-nm layer of nickel oxide was sputter-deposited followed by annealing at 300 °C in air for 10 minutes. The remaining fabrication steps were all performed in an inert atmosphere inside nitrogen glove boxes. Samples were sealed in a nitrogen-filled container for any transfer between glove boxes. A 2 mg/mL solution of PTAA was spin coated on to the nickel oxide layer at 6,000 rpm for 30 s followed by a 10 minute anneal at 100 °C on a hotplate. The $FA_{0.87}MA_{0.08}Cs_{0.05}Pb(I_{0.92}Br_{0.08})_3$ precursor solution was prepared by dissolving 1.3 M Pb^{2+} in 1-methyl-2-pyrrolidinone (NMP) and dimethylformamide (DMF) (v/v = 12/88) mixed solvent. Perovskite films were spin coated with a two-step, nitrogen quench process with the first step of 2,000 rpm for 10 s followed by 6,000 rpm for 24 s where a nitrogen jet is applied to the surface for 15 s beginning 1 s into the second step. The deposited film was then annealed for 30 minutes at 100 °C on a hotplate. Sequential layers of C_{60} (25 nm), bathocuproine (6 nm), and silver (100 nm) are thermally evaporated onto the perovskite to complete the device.

Device characterization

J-V measurements were taken in a N2 glovebox. Illumination was provided with a xenon arc lamp and calibrated to 1-sun intensity. A small fan was directed over the substrate to mitigate heating from illumination. *J-V* scans were taken with a Keithley 2450 source-measure unit. Sweeps were taken from -0.2 V to 1.2 V at a rate of 0.8 V/s. Cells were allowed to light-soak until a steady-state was reached as determined by successive reverse sweeps. Following the reverse sweeps, at least 3 forward sweeps were performed to verify a stabilized measurement.

Device stability

Solar cells without any encapsulation were loaded into a custom degradation testing setup, dubbed the Stability Parameter Analyzer (SPA) systems. The aging systems consist of a flow chamber to control the environment of the cells; electrical housing and electronics that switch between devices, measure *J-V* curves, and hold the devices under resistive load; and a light source that provides constant illumination. One of the SPA systems uses a sulfur plasma lamp for illumination at 0.77 Suns and the other system uses light emitting diode illumination for 1.2-Suns illumination. In this study, devices were kept in an N_2 environment and held under a resistive load of 510 Ω (placing the cells near maximum power point). A substrate temperature of 55 °C, 65 °C, or 70 °C was maintained with a closed water loop through the mounting block. Approximately every 75 minutes, the system removes the resistive load and takes a *J-V* scan using a Keithley 2450 source-measure unit. Figures of merit were calculated from the in-situ *J-V* sweeps and used to evaluate performance. Pixels that demonstrated a system-level contact issue were excluded from analysis.

Device modeling.

Devices were modeled in COMSOL as a simple diode sandwiched between an ITO electrode and a C_{60}/BCP and silver pad electrode using a current continuity model considering conduction in the ITO, the C_{60}/BCP, and the silver layers. Photocurrent and diode current density at each location (*x*, *y*) in the simulation was simulated using the equation below, where j_{photo} depends on whether the location was inside or outside of the illuminated area in the case of a simulation of a masked device. For unmasked device simulations, j_{photo} was independent of *x* and *y*.

$$j_{diode}(x,y) = j_0\left(e^{\frac{q(V_{top}(x,y) - V_{bottom}(x,y))}{nkT}} - 1\right) - j_{photo}(x,y)$$

This equation acts like a current source term in the top and bottom electrode assemblies. The outside edges of the ITO electrode away from the side of the silver pad were kept at ground (Figure S1). The voltage was applied to the furthest edge. Lateral currents in the top and bottom layers were simulated using Ohm's laws.

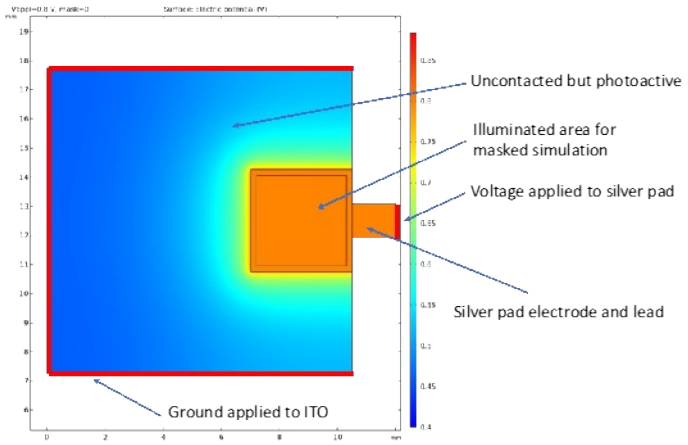

Figure S1. COMSOL simulation layout. The ITO extends behind the large square on the left. The top silver electrode is approximate 3.5x3.5 mm and has a contact pad extending to the right. Illumination occurs in the smaller masked square inside the pad area for masked device simulations.

Supplementary Table and Figures

Table S1. List of materials and treatments for PSC design examined in this work.

Layer	Variants
Active Layer Materials	$FA_{0.87}Cs_{0.13}Pb(I_{0.92}Br_{0.08})_3$
	$FA_{0.87}MA_{0.13}Pb(I_{0.92}Br_{0.08})_3$
	$FA_{0.64}MA_{0.20}Cs_{0.15}Pb(I_{0.80}Br_{0.2})_3$
	$FA_{0.87}MA_{0.08}Cs_{0.05}Pb(I_{0.92}Br_{0.08})_3$
	$FA_{0.83}Cs_{0.17}PbI_3$
	$FA_{0.87}Cs_{0.13}Pb(I_{0.95}Br_{0.05})_3$
Active Layer Modifications	Potassium thiocyanate (KSCN)
	Indium(III) bromide ($InBr_3$)
	Single Crystal Precursor
	Formamidinium iodide
	Gallium(III) acetylacetonate ($Ga(AcAc)_3$)
	Dimethyl sulfoxide (DMSO)
	Lead(II) iodide (PbI_2)
	Lead(II) chloride ($PbCl_2$)
	1-Butyl-3-methylimidazolium tetrafluoroborate (BMIM:BF_4)
	Carbon tetrachloride (CCl)
	Methylammonium chloride (MACl)
	Dipropylsulfoxide (DPSO)
	1-Butyl-3-methylimidazolium hexafluorophosphate (BMIM:PF_6)
	Methylammonium thiocyanate (MASCN)
	Cesium bromide (CsBr)
	Magnesium acetylacetonate ($Mg(AcAc)_2$)
	Y6
	Butylamine
	PEA_2PbI_4
	D-4-tert-butylphenylalanine (D4TBP)
	1,3-Dimethyl-2-oxohexahydropyrimidine, N,N'-Dimethylpropylene urea (DMPU)
	Phenethylammonium iodide (PEAI)
	4-fluorophenylethylammonium (4F-PEA)
	Lead diethyldithiocarbamate ($Pb(DDTC)_2$)
	Potassium iodide (KI)
	4F-PEA_2PbI_4
	Oleylamine (OAm)
	Methylammonium iodide (MAI)
	Methyl Acetate (MeOAc)
	5-fluorophenylethylammonium (5F-PEAI)
	Tetradecyldimethyl (3-sulfopropyl)ammonium hydroxide inner salt (TAH)
	Triphenylphosphine oxide (TPPO)
	Formamidinium iodide (FAI)
	4-Fluorophenylethylammonium iodide (4F-PEAI)
	1-Butyl-1-methylpyrrolidinium tetrafluoroborate (BMP BF_4)
	Phenylacetic acid (PA)
	Lead(II) thiocyanate ($Pb(SCN)_2$)
	1-Butyl-2,3-dimethylimidazolium tetrafluoroborate (BDMIM:BF_4)
	Methylammonium lead chloride (MAPbCl3)
	Guanadinium bromide (GABr)
	Formic Acid

Table S1 (cont.). List of materials and treatments for PSC design examined in this work.

Layer	Variants
HTL Modifications	4-Fluorophenylethylammonium iodide (4F-PEAI)
	N4,N4'-Di (naphtha len-1-y l)-N4,N4'-bis (4-viny lpheny l)bipheny l-4,4'-diamine (VNPB)
	Dodecylammonium iodide (DDAI)
	Oxygen Plasma
	1-Butyl-3-methylimidazolium tetrafluoroborate (BMIM:BF_4)
	Potassium Chloride (KCl)
	[2-(3,6-Dimethoxy-9H-carbazol-9-yl)ethyl]phosphonic Acid (MeO-2PACz)
ETL Materials	Bathocuproine (BCP)
	Fullerene-C_{60} (C_{60})
	Tin oxide (SnOx)
	Lithium flouride (LiF)
ETL Modifications	4-Fluorophenylethylammonium iodide (4F-PEAI)
Electrode	Indium-doped zinc oxide (IZO)
	Gold (Au)
	Copper (Cu)
	Tantalum (Ta)
	Silver (Ag)
	Indium-doped tin oxide (ITO)

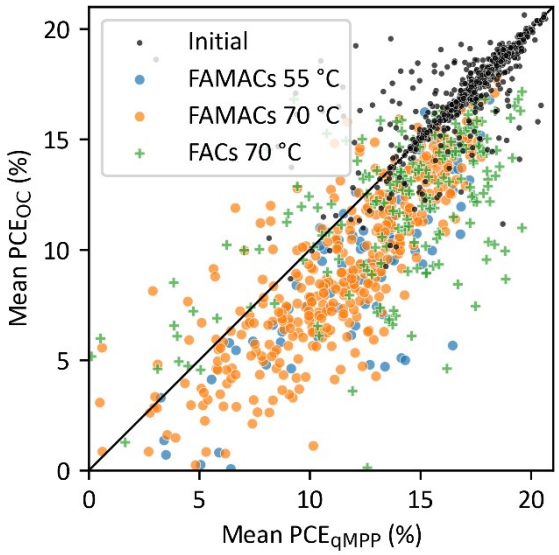

Figure S2.Mean PCE of OC devices vs. qMPP devices for all devices in this study. Initial (i.e., pre-aging) data are shown in black while post-aging data are shown in blue, orange, and green. A one-to-one parity line is shown for reference.

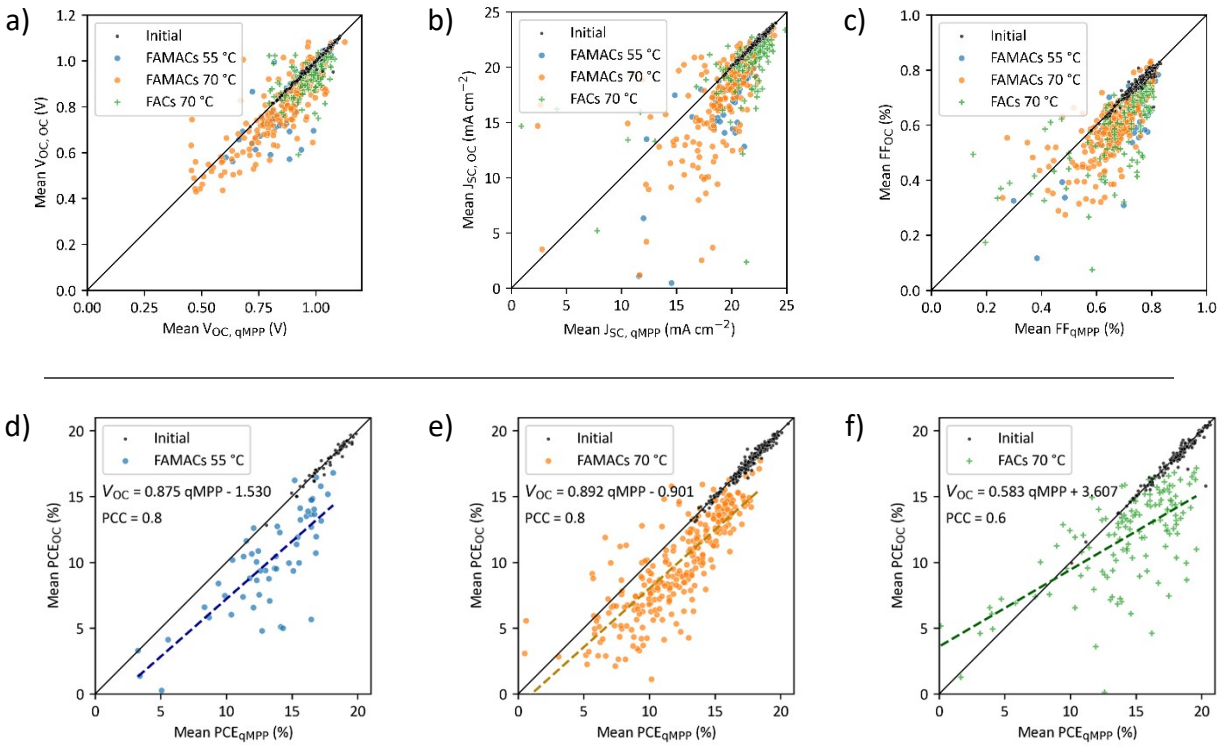

Figure S3. Mean value of OC devices vs. qMPP devices for (a) V_{OC}, (b) J_{SC}, and (c) FF. PCE for MHP groupings are shown in d-f with data trend lines and Perason correlation coefficient (PCC). Initial (i.e., pre-aging) data are shown in black while post-aging data are shown in blue, orange, and green. A one-to-one parity line is shown for reference.

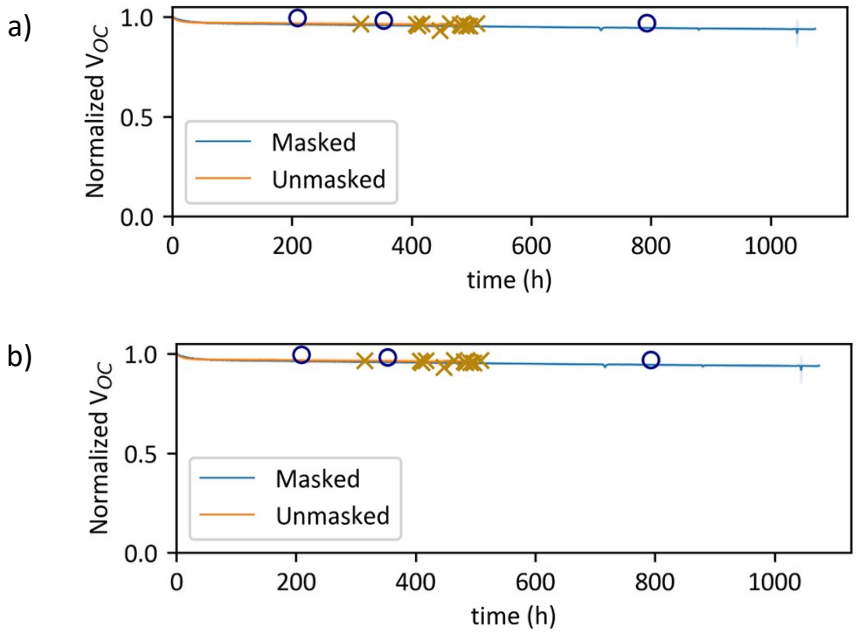

Figure S4. Normalized (a) V_{OC} and (b) FF of devices during aging. X and O markers in the plots indicate the time and final figure of merit value of devices before device dropout or step-edge failure, respectively.

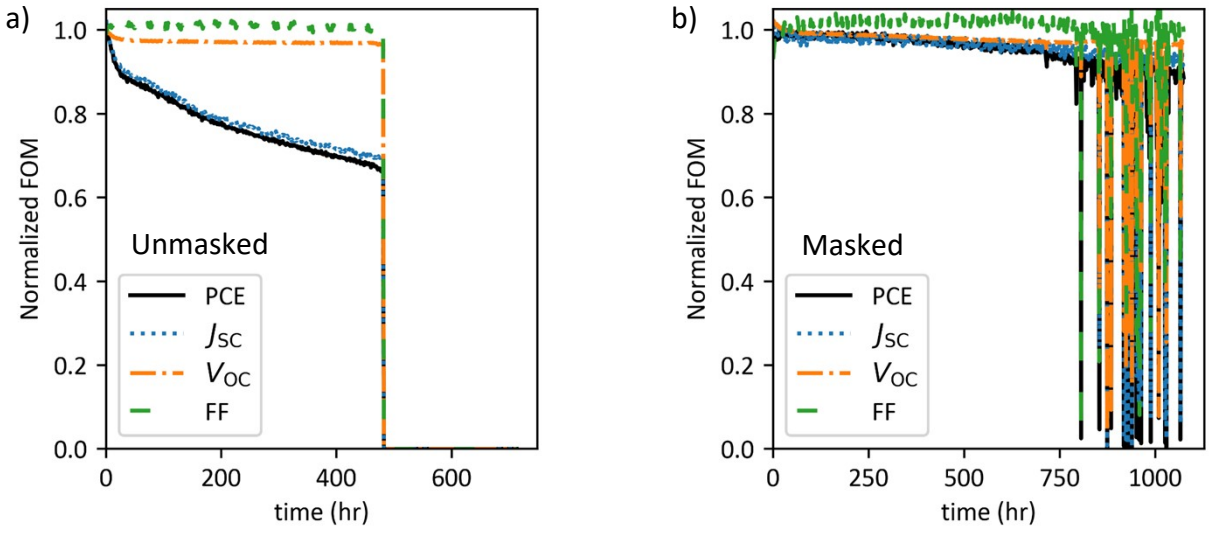

Figure S5. Normalized FOMs of an (a) unmasked and (b) masked device during aging.